Journal of Superconductivity and Novel Magnetism

Special Issue Dedicated to Jacques Friedel on the Occasion of His 90th Birthday

Volume 25 · Number 3
April 2012

10948 · ISSN 1557-1939
25(3) 547–722 (2012)

Springer

Superconductivity and the Van Hove Scenario

Julien Bok & Jacqueline Bouvier

Journal of Superconductivity and Novel Magnetism
Incorporating Novel Magnetism

ISSN 1557-1939
Volume 25
Number 3

J Supercond Nov Magn (2012)
25:657-667
DOI 10.1007/s10948-012-1434-3

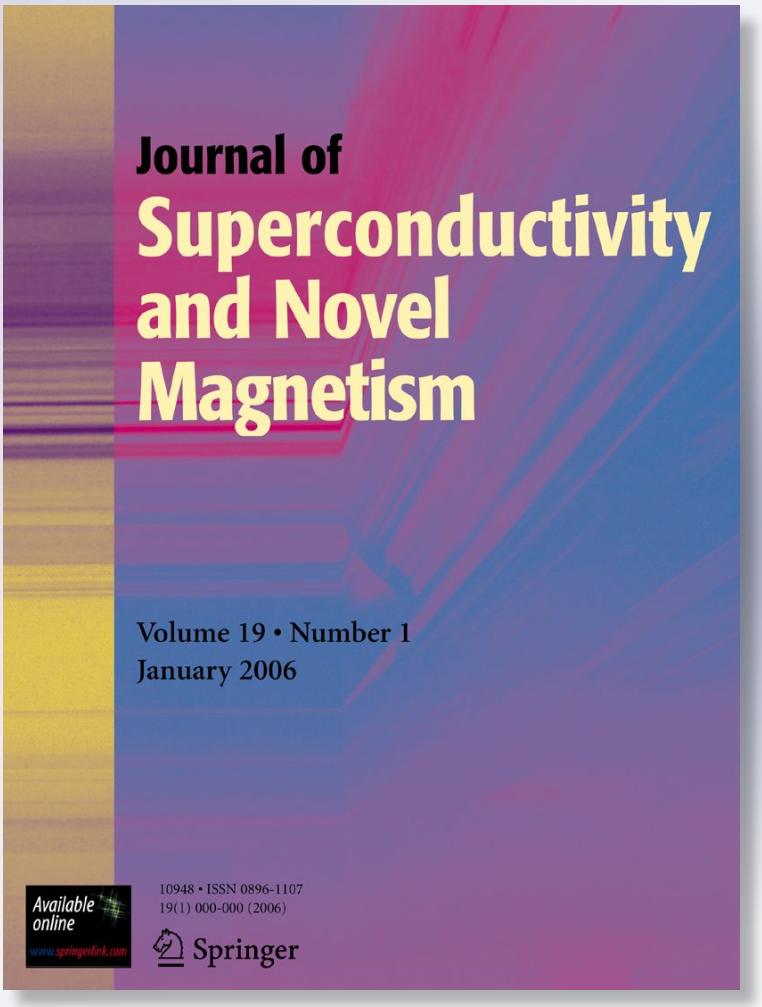

Springer

J Supercond Nov Magn (2012) 25:657–667
DOI 10.1007/s10948-012-1434-3

SUPERCONDUCTIVITY

Superconductivity and the Van Hove Scenario

Julien Bok · Jacqueline Bouvier

Received: 9 January 2012 / Accepted: 10 January 2012 / Published online: 10 February 2012

Abstract We give a review of the role of the Van Hove singularities in superconductivity. Van Hove singularities (VHs) are a general feature of low-dimensional systems. They appear as divergences of the electronic density of states (DOS). Jacques Friedel and Jacques Labbé were the first to propose this scenario for the A15 compounds. In NbTi, for example, Nb chains give a quasi-1D electronic structure for the d-band, leading to a VHs. They developed this model and explained the high T_C and the many structural transformations occurring in these compounds. This model was later applied by Jacques Labbé and Julien Bok to the cuprates and developed by Jacqueline Bouvier and Julien Bok. The high T_C superconductors cuprates are quasi-bidimensional (2D) and thus lead to the existence of Van Hove singularities in the band structure. The presence of VHs near the Fermi level in the cuprates is now well established. In this context we show that many physical properties of these materials can be explained, in particular the high critical temperature T_C, the anomalous isotope effect, the superconducting gap and its anisotropy, and the marginal Fermi liquid properties, they studied these properties in the optimum and overdoped regime. These compounds present a topological transition for a critical hole doping $p \approx 0.21$ hole per CuO_2 plane.

Keywords Superconductivity · High T_C · Van Hove scenario · Density of states

J. Bok (✉) · J. Bouvier
ESPCI Paris Tech, 10, rue Vauquelin, 75231 Paris Cedex 05, France
e-mail: julien.bok@espci.fr

J. Bouvier
e-mail: jacqueline.bouvier@espci.fr

1 Introduction

After World War II, Solid State Physics was practically non-existent in France. Two places were at the origin of a revival of the field, Ecole Normale Supérieure (ENS) in Paris with Pierre Aigrain and the University of Orsay with Jacques Friedel, André Guinier and Raymond Castaing.

A postgraduate course was also created in the Parisian areas called "troisième cycle" in Solid State Physics. There were two poles, one in Orsay with J. Friedel and A. Guinier later joined by Pierre-Gilles de Gennes and another at ENS with P. Aigrain, later replaced by J. Bok.

The great majority of solid state physicists working in France are former students of this DEA (Diplôme d'Etudes Approfondies). One of the authors (J. Bok) is very grateful to J. Friedel for his constant confidence. We collaborated for more than 30 years in maintaining a very high level in this research school in solid state physics.

In this paper we shall review the work of Labbé, Friedel and Barišić on the A15 and our work on cuprates in the framework of the Van Hove scenario.

2 Friedel et al. Work on Supraconductivity and Van Hove Singularity

The original approach of Friedel et al. is the following: The elastic properties of most metals and metallic compounds are generally weakly dependent on temperature. In the A_3B (V_3Si, Nb_3Sn), called A15 compounds, on the other hand relatively high superconducting critical temperatures T_C (16–18 K) are observed simultaneously with structural instabilities. This fact, coupled especially with the occurrence among these same materials of structural phase

transformations known to involve lattice vibrational instabilities, has created a lively interest in the lattice dynamics and in particular the nature of electron–phonon interaction in materials with this structure. The basic idea, first proposed by Labbé and Friedel and since elaborated by various authors, is that one is dealing with a nearly empty set of d-electron bands whose degeneracy is removed by the elastic strain. The re-equilibration of the electrons within the split bands of the strained structure can in favorable conditions balance the normal increase in elastic energy. This destabilizing d-electron contribution is one, however, which increases with decreasing temperature as the Fermi surface becomes sharper.

From the 1960s to the 1980s Jacques Friedel was collaborating with Jacques Labbé, and Slaven Barišić [1–15, 19]. They studied the instability of the cubic phase of intermetallic compounds of the type V_3Si at very low temperature. There idea was that a Jahn–Teller type of effect for the d-band electrons can explain this instability. When the temperature is raised the effect is reduced and above a certain temperature T_M, it is compensated by the action of the conduction electrons, which can reasonably be supposed to stabilize the cubic phase. It is at this temperature T_M that the change of structure from tetragonal-to-cubic phase occurs. They explained the martensitic transition observed at low temperature in experiment.

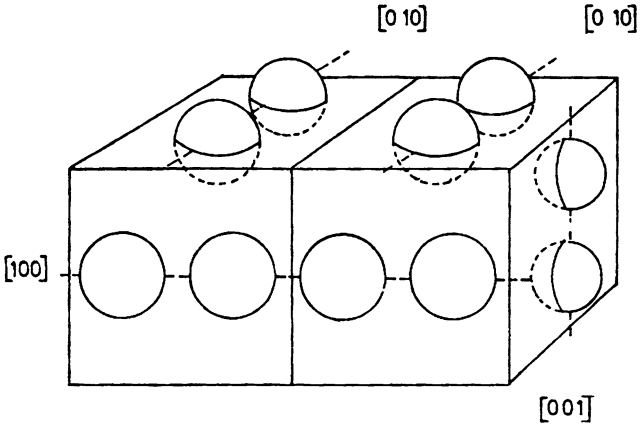

Fig. 1 The A15 crystal structure: the spheres represent vanadium atoms; the Si atoms would be at the corner and at the center of the cube

At absolute zero temperature the Fermi level is supposed to lie in a region of quickly changing density of states. The deformation of the crystal reduces the degeneracy of the electron spectrum and a large change of the DOS occurs at the Fermi level. For a certain range of initial Fermi level positions this can be accompanied by the decrease of the free energy and thus by a phase transition. Furthermore such a situation will be temperature sensitive; thus one can expect a strong temperature dependence of the associated quantities, in particular of the coefficients in the series expansion of the free energy in terms of the strains of the cubic lattice.

In their model they used arbitrary values for the DOS at the Fermi level and for the bandwidth, but the lattice parameters, the shear modulus, and the variation of the elastic constant with temperature were taken from experiments [16, 17]. They concluded in favor of a first order transition.

d-electrons, moving along the dense vanadium chains, are treated in the tight-binding approximation. In the cubic phase the vanadium atoms are arranged in chains stretching in the [100], [010] and [001] directions (Fig. 1). They write a self-consistent potential V for vanadium *d*-electrons, and calculate the DOS corresponding to the single-chain energy contribution, this leads to a very high peak in the DOS. The Fermi level should fall in one of these peaks. The value of n(E) (DOS) is infinite at the edges of a d-sub-band Fig. 2. The width of this peak is much smaller than the width $\hbar\omega_D$ of the phonon spectrum. A tetragonal distortion could make the energy decrease, when the Fermi level (FL) was sufficiently close to a peak. In such a distortion, the degeneracy is partly lifted, each peak splitting into two peaks. In V_3Si, the stable phase, at absolute zero, is tetragonal, FL lies between two high peaks (Fig. 3). The rather fine structure is very sensitive to temperature. By an increase in the temperature, the occupancy of a high peak becomes appreciable, this leads to a decrease in the stability of the tetragonal phase (Figs. 4, 5). A variation of the distortion parameter ϵ occurs.

Among other properties, this leads to a large and strongly temperature-dependent Pauli susceptibility, Knight shift, which were studied and calculated by J. Labbé [8, 9].

In the framework of the BCS theory, J. Labbé, S. Barišić and J. Friedel [6] calculated the critical superconducting temperature T_C and the superconducting gap Δ, using their

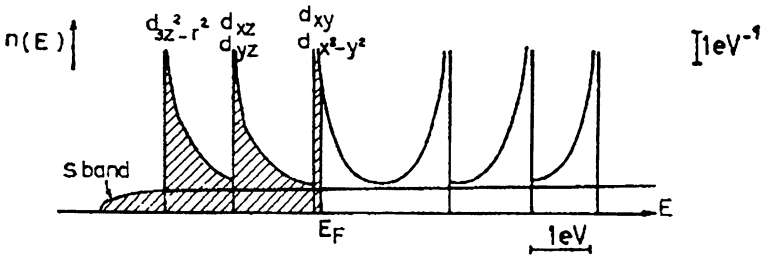

Fig. 2 Density of states (DOS) in the tetragonal phase, calculated in the tight-binding model

high DOS at FL in the normal state at the bottom of the d-sub-band. T_C and Δ vary with the small number of electrons in the narrow d-sub-band. The limit of integration becomes $-\hbar\omega_D$ to $+\hbar\omega_D$. They conclude that they can expect among the A_3B type compounds the situation between strong and weak coupling limit of superconductivity (Fig. 6), with more or less negligible isotopic effect.

In the 1980s, the discovery of high critical superconducting temperature in layered-metal oxides $T_C = 35$ K, as $La_{2-x}A_xCuO_4$ (A = Ba, Sr), by Bednorz and Müller [18] raised once again the questions concerning the interplay between the structural and the superconducting instabilities. These new superconductors are tetragonal. But La_2CuO_4 is orthorhombic at ambient temperature and shows a metal-to-insulator transition below 100 K, and with the doping x. The properties of these materials come essentially from the CuO_2 plane. Friedel et al. [19] proposed a simple electron-phonon model for these new compounds. The predictions of the model are the tetragonal-to-orthorhombic instability and separately from it, the bond dimerization within the layers. The high T_C in those materials is associated with the soft shear branch in their tetragonal state, the main contribution to the electron-phonon coupling in ionic metals is attributed to the deformation-induced variation of the crystal field on the ionic sites which are involved in conduction.

The work of Friedel et al. is very unique and profound. It gave a good description of the properties of the A15 and it opened a new approach of superconductivity which was later developed by a new generation of researchers.

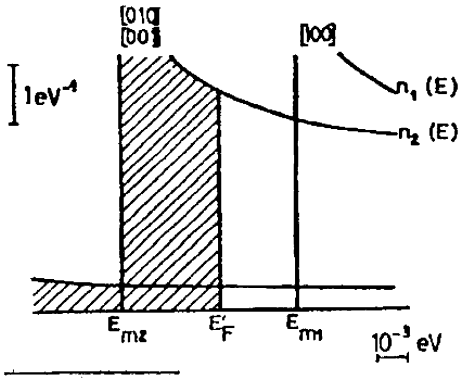

Fig. 3 Fermi level position in the tetragonal phase of V_3Si

3 VHs Physics in 1, 2, 3 Dimensions—Electronic Structure of the Cuprates

Van Hove singularities [20] are general features of periodic systems. They are topological properties of the electronic band structure (BS) and do not depend on the particular form of the BS. In one dimension (1D), they give a divergence of the DOS varying as $1/(E - E_S)^{1/2}$, where E_S is the energy of the singularity level. In two dimensions (2D), a one electron calculation is easy to perform, a general feature of a 2D model is the presence of VHs with logarithmic divergence of the DOS at an energy $E = E_S$ [21]. Near VHs the variation of the DOS is logarithmic varying as $\ln(D/(E - E_S))$ (Fig. 7) where $D/2$ is the width of the singularity. In three dimensions (3D) the divergence is removed and we have a truncated 2D DOS.

It is now well accepted that the origin of cuprate superconductivity is to be found in the CuO_2 planes, which are weakly coupled together in the c direction, so that their electronic properties are nearly two dimensional. There were examples of superconducting cuprates with high T_C to which we applied our model: $Bi_2Sr_2CaCu_2O_8$ (Bi 2212), $YBa_2Cu_3O_7$ (Y123), $YBa_2Cu_4O_8$ (Y124) and $Nd_{2-x}Ce_xCuO_{4+\delta}$ (NCCO). For low oxygen content (no doping) all copper ions in this plane are Cu^{++} ions, the material is an anti-ferromagnetic insulator due to strong electron-electron repulsion on the same copper site. With additional oxygenation or doping, holes are introduced in the CuO_2 planes and the compound becomes conducting and superconducting for $T < T_C$. The maximum T_C is achieved when the hole content is around 16% per Cu atom.

More advanced calculation, using the band structure of (2), gives the result shown in Fig. 8 for the constant energy surfaces (CES) in k-space [22, 23]. This is very well confirmed by the results of Ino [24] using angular resolved photoemission spectroscopy (ARPES) (see Fig. 7 of Ref. [24]). A topological transition is well seen for a doping value $p_c = 0.21$ hole per Cu atom. The CES are hole-like for $p < p_c$ and electron-like for $p > p_c$. The resulting VHs is shown in Fig. 9, and thus increases the transition temperature whatever the pairing mechanism. The main consequences of this Van Hove scenario are given in Refs. [22, 23].

This approach is not valid for the underdoped region. The strong Coulomb repulsion U between two electrons on

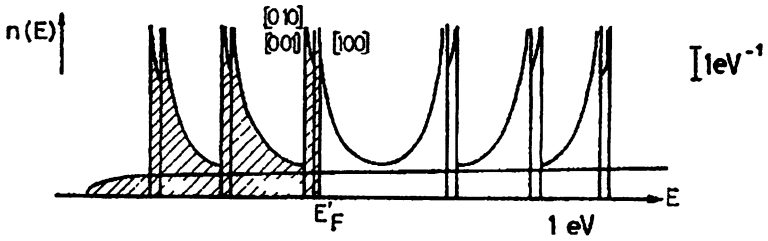

Fig. 4 Density of states in the cubic phase, calculated in the tight-binding model

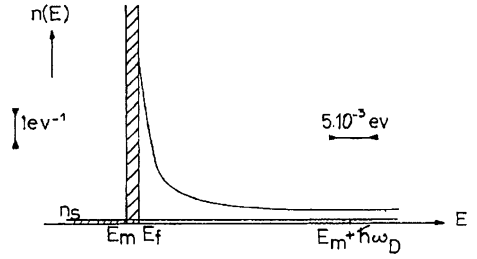

Fig. 5 Density of states and Fermi level position in the normal state

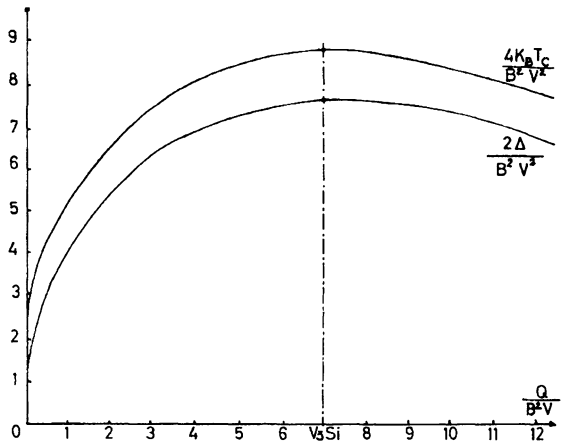

Fig. 6 Variations of the gap and the superconducting transition temperature with small number of electrons in the narrow d sub-band

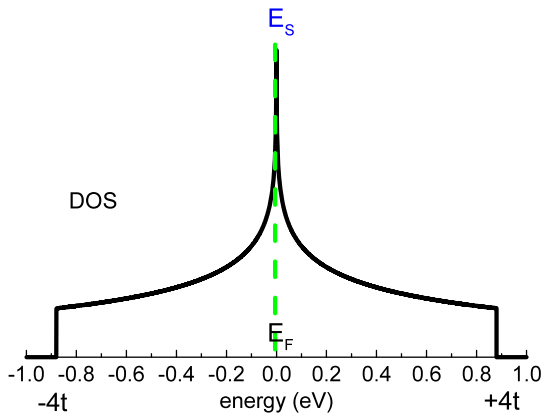

Fig. 7 Density of states of a 2D system ($E_F \equiv$ FL)

a same site is responsible for the fact that with $p = 0$ the cuprates are Mott insulators with antiferromagnetic (AF) order. The AF order disappears rather rapidly with doping, but AF fluctuations remain, and decrease, until the optimum doping. This region of strong correlations is present and the valid approach is that of a doped Mott insulator [25]. This is also seen in ARPES; some points of the Fermi surface disappear for underdoped samples.

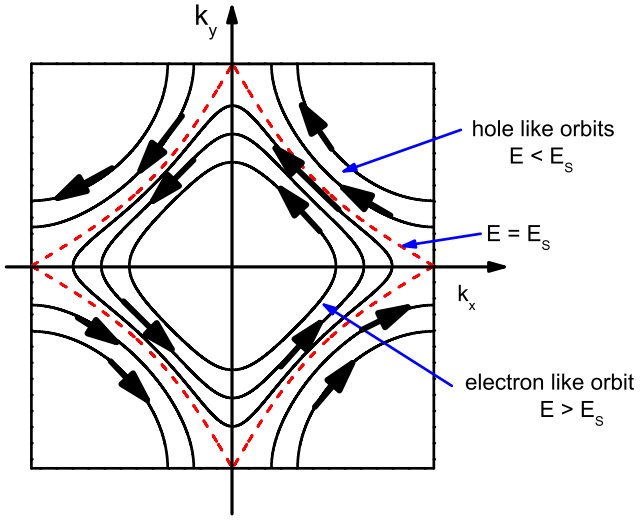

Fig. 8 Constant energy surfaces

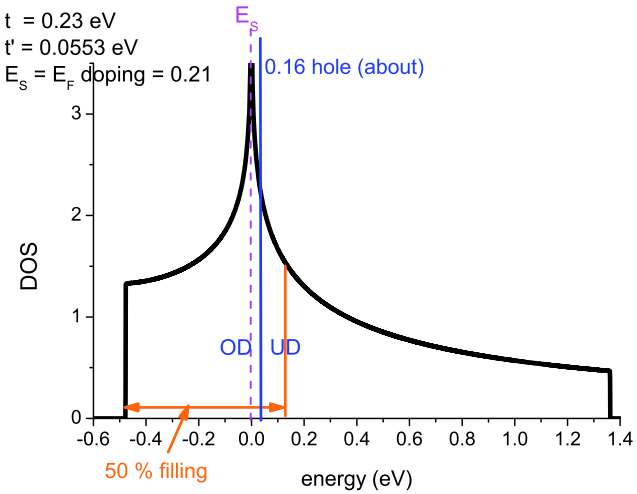

Fig. 9 Density of states

4 Calculation of T_C with Electron–Phonon Interaction

4.1 Calculation of T_C Using the BCS Approach

Labbé–Bok (1987) [21] have computed the band structure for the bidimensional CuO_2 planes of the cuprates, considered as a square lattice (quadratic phase). They obtained a formula for T_C using the following assumptions:

1. The Fermi level lies at the Van Hove singularity.
2. The BCS approach is valid:
   - The electron–phonon interaction is isotropic and so is the superconducting gap Δ.
   - The attractive interaction V_p between electrons is non-zero only in an interval of energy $\pm\hbar\omega_0$ around the Fermi level where it is constant. When this attraction is mediated by emission and absorption of phonons, ω_0 is a typical phonon frequency.

In that case, the critical temperature is given by

$$k_B T_C = 1.13 D \exp\left[-\left(\frac{1}{\lambda} + \ln^2\left(\frac{\hbar\omega_0}{D}\right) - 1.3\right)^{1/2}\right] \quad (1a)$$

where λ is the electron-phonon coupling constant [4].

A simplified version of formula (1a), when $\hbar\omega_0$ is not too small compared to D, is

$$k_B T_C = 1.13 D \exp\left(-1/\sqrt{\lambda}\right). \quad (1b)$$

The two main effects enhancing T_C are

1. The prefactor in formula (1b) which is an electronic energy much larger than a typical phonon energy $\hbar\omega_0$.
2. λ is replaced by $\sqrt{\lambda}$ in formula (1b) in comparison with the BCS formula, so that in the weak coupling limit when $\lambda < 1$, the critical temperature is increased.

As it is, however, this approach already explains many of the properties of the high T_C cuprates near optimum doping.

4.2 The Variation of T_C with Doping

Then we did more accurate calculations (1995–1997) [26, 27]. By taking into account the repulsive interaction between second nearest neighbors (s.n.n.), and the variation of hole doping [26], the band structure becomes

$$E_k = -2t(\cos X + \cos Y) + 4t' \cos X \cos Y + D_e \quad (2)$$

where t' is an integral representing the interaction with s.n.n., where $D_e = E_F - E_S + (4t')$ represents the doping in hole p. The Fermi surface at the VHs is no longer a square but is rather diamond-shaped, Fig. 8, and we obtain the DOS of Fig. 9. For lower or higher doping the critical temperature decreases. We adjusted the experimental results of Koïke et al. [28], Fig. 10. In this case the authors varied the hole concentration in the CuO_2 planes of $Bi_2Sr_2CaCu_2O_{8+\delta}$ using different substitution of cations with different valences, obtaining different systems, i.e.: $Bi_2Sr_2Ca_{1-x}Lu_xCu_2O_{8+\delta}$, $Bi_2Sr_2Ca_{1-x}Na_xCu_2O_{8+\delta}$, $Bi_2Sr_{2-x}Ca_{1-x}La_xCaCu_2O_{8+\delta}$, $Bi_2Sr_{2-x}K_xCaCu_2O_{8+\delta}$. In this figure our model account for the variation of the holes in the CuO_2 plane, from an optimum doping, here $p \approx 0.20$, of this group of compounds, and we calculate the corresponding T_C when E_F shifts from E_S.

4.3 Influence of the Coulomb Repulsion

Although BCS theory [29] neglects Coulomb repulsion, Anderson and Morel [30] showed very early that it plays a central role in superconductivity. Assuming a constant repulsive potential V_C from 0 to E_F, they found that T_C is given by

$$T_C \cong T_0 \exp\left[\frac{-1}{\lambda - \mu^*}\right] \quad (3)$$

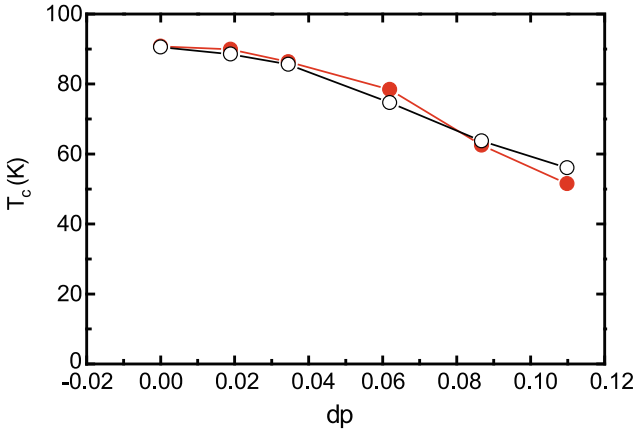

Fig. 10 Comparison of the variation of T_C with the variation of the doping dp from the optimum doping at $dp = 0$, calculated in our model (*filled circles*) and the experimental results of Koïke et al. (*open circles*) [28]

with

$$\mu = N_o V_C \quad \text{and} \quad \mu^* = \frac{\mu}{1 + \mu \ln E_F/\omega_0}.$$

Cohen and Anderson [31] assumed that for stability reasons μ is always greater than λ. Ginzburg [32] gave arguments that in some special circumstances μ can be smaller than λ. Nevertheless if we take $\mu \geq \lambda$, superconductivity only exists because μ^* is of the order of $\mu/3$ to $\mu/5$ for a Fermi energy E_F of the order of 100 $\hbar\omega_0$. It is useless to reduce the width of the band W, because λ and μ vary simultaneously and μ^* becomes greater if E_F is reduced, thus giving a lower T_C. Superconductivity can even disappear in a very narrow band if $\lambda - \mu^*$ becomes negative.

Force and Bok studied the renormalization of μ, in the case of a peak in the DOS in the middle of a broad band [33]. They predict a high T_C in this case due to three main effects:

- $(\lambda - \mu^*)$ is replaced by the square root $(\lambda - \mu^*)^{1/2}$.
- μ^* is reduced compared to μ because the renormalization is controlled by the width W of the broad band and not the singularity.
- The prefactor before the exponential in the formula giving T_C is the width of the singularity D instead of the phonon energy $\hbar\omega_0$.

In Fig. 11, we show the variation of T_C with the width of the singularity D, all others parameters (W, ω_0) remaining constant.

5 Anomalous Isotope Effect

The variation of T_C with the mass M of the atom of the metal is considered as evidence for electron–phonon interaction as the origin of pairing. In this BCS model [29] T_C varies

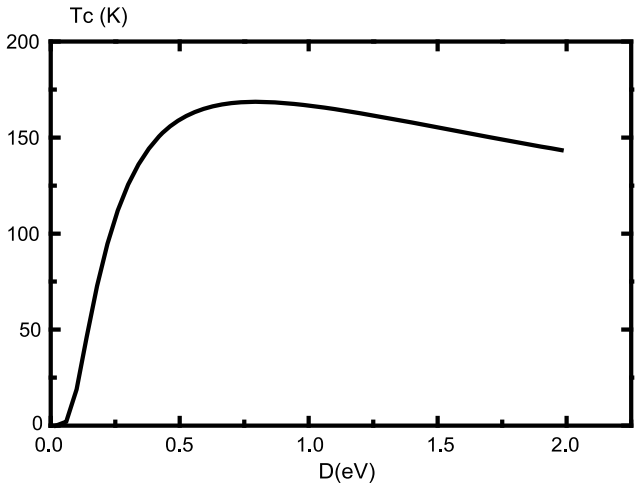

Fig. 11 Effect of the band width D of the singularity on T_C

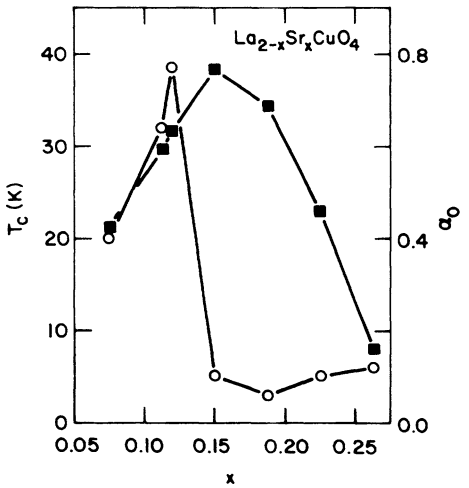

Fig. 12 From Ref. [37], experimental results of T_C(■) and α(●) as a function of doping concentration for $La_{2-x}Sr_xCuO_4$ (the data were taken from Ref. [35])

as $M^{-1/2}$. The almost complete absence of the isotope effect when O^{18} was substituted to O^{16} in the cuprates [34] was considered as evidence for the non-phonon origin of superconductivity. But Labbé–Bok [21], using formula (1a), have shown that the isotope effect is strongly reduced for HTCS cuprates at optimum doping. This is due to the fact that in this situation the Fermi level lies near the VHs and then the width of the singularity D is more important than the phonon frequency ω_0. They also have predicted that the isotope effect should reappear for underdoped samples. This was later experimentally observed [35, 36]. The isotope effect may be measured by the coefficient α defined as T_C proportional to $M^{-\alpha}$ ($\alpha = 0.5$ for usual superconductors). Tsuei et al. [37], using the VH scenario, have calculated the variation of α with doping and have shown that it explains the experimental observations, Fig. 12.

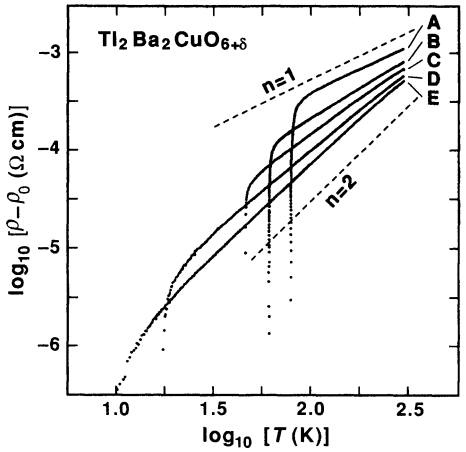

Fig. 13 From Ref. [43], fit of the resistivity ρ of $Tl_2Ba_2CuO_{6+\delta}$ to a power law temperature dependence $\rho = \rho_0 + AT^n$ shown on a log–log scan. The *dashed lines* indicate the slope for $n = 1$ and $n = 2$

6 Non-Fermi Liquid Properties

6.1 Resistivity

In a classical Fermi liquid, the lifetime broadening $1/\tau$ of an excited quasiparticle goes as ε^2 and the resistivity ρ varies as T^2. The marginal Fermi liquid situation is the case where $1/\tau$ goes as ε (electronic energy) and ρ is linear in T. In the half-filled nearest-neighbor coupled Hubbard model on a square lattice, Newns et al. [38, 39] have shown that this can also occur when E_F is close to E_S. This calculation was, however, contradicted by Hlubina and Rice [40].

Experimental evidence of marginal Fermi liquid behavior has been seen in angle resolved photoemission [41], infrared data and temperature dependence of electrical resistivity [42]. Marginal Fermi liquid theory, in the framework of VHs, predicts a resistivity linear with temperature T. This was observed by Kubo et al. [43] and cited in Ref. [25]. They also observe that the dependence of resistivity goes from T for high T_C material to T^2 as the system is doped away from the maximum T_C, Fig. 13, which is consistent with our picture; in lower T_C material the Fermi level is pushed away from the singularity.

6.2 Hall coefficient

Many measurements of the Hall coefficient R_H in various high T_C cuprates have been published [44, 45]. The main results are the following:

(i) At low temperature T, $R_H \approx 1/p_{h0}e$, where p_{h0} is the hole doping, when T increases R_H decreases, and for highly overdoped samples becomes even negative.
(ii) These authors are also able to define a temperature T_0, where R_H changes its temperature behavior, and they found that $R_H(T)/R_H(T_0)$ versus T/T_0 is a universal

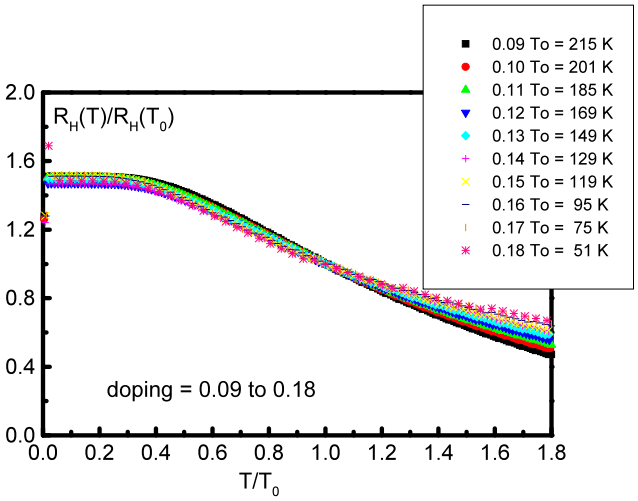

Fig. 14 Universal law $R_H(T)/R_H(T_0)$ versus T/T_0 for various hole doping levels, from 0.09 to 0.18

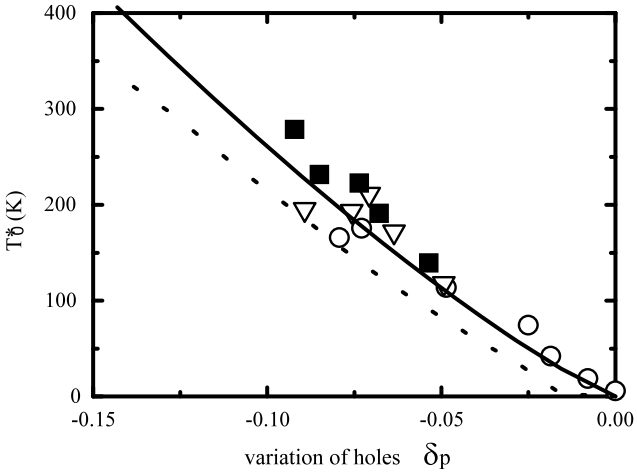

Fig. 15 The temperature, T_0, where the calculated χ_p (*dashed line*) and the specific heat (*solid line*) go through a maximum, versus δp. For comparison we show the results presented in Fig. 27 of Ref. [49], the symbols are the same (*solid squares*: from thermoelectric power, *circles*: from specific heat, *triangles*: from NMR Knight shift data)

curve for a large doping domain (from $p_{h0} = 0.10$ to $p_{h0} = 0.27$).

We can explain [46], following the approach given by Ong [47], these results by using the band structure for carriers in the CuO_2 planes. In particular, the existence of hole-like and electron-like constant energy curves, Fig. 8, which give contributions of opposite sign to R_H. The critical doping, for which a topological transition is observed and calculated is $p = 0.21$ hole per CuO_2 plane. The transport properties explore a range of energy $k_B T$ around the Fermi level, when T is increased more and more carriers are on the electron-like orbits, resulting in a decrease of R_H. In Ref. [46] we present our calculations and the theoretical fits of many experimental results, and we show that it works and this supports our model. We find the universal law (Fig. 14).

6.3 Specific Heat and Electronic Susceptibility

Several experiments on photoemission, NMR and specific heat have been analyzed using a normal state pseudogap [48]. In fact, all that is needed to interpret these data is a density of state showing a peak above the Fermi energy. To obtain the desired DOS several authors [48] introduce a pseudogap in the normal state. This seems to us rather artificial, the above authors themselves write that the physical origin of this pseudogap is not understood. We have shown that by using a band structure of the form of formula (2), we may interpret the results obtained in the normal metallic state.

The variation with the doping is linked to the distance of the FL from the singularity level ($E_F - E_S$), so does the variation with the temperature due to the Fermi–Dirac distribution.

We find a characteristic temperature T_0 where the variation of the electronic susceptibility χ_p versus T goes through a maximum. We may express $D_e = E_F - E_S$ as a variation of doping $\delta p = p - p_0$, p_0 being the doping for which $E_F = E_S$, $p_0 = 0.20$ hole/copper atom in the CuO_2 plane.

We have also computed the electronic specific heat C_s [27] in the normal state using the same DOS. We find that $\gamma = C_s/T$ goes through a maximum with temperature T, at a value T^* as found experimentally by Cooper and Loram [49]. In Fig. 15 we compare our computed T_0 with the experimental one (Ref. [49]); the agreement is excellent. So we are able to interpret the NMR and specific heat data in the normal metallic state without invoking a pseudogap, but simply by taking into account the logarithmic singularity in the DOS. The existence of a pseudogap is however well established in the underdoped regime.

We also explain the shift between the observed experimental optimum T_C, where $p = 0.16$ instead of 0.20, and the expected optimum T_C from our theory, i.e. where $D_e = 0$, by the fact that at first in our gaps calculations we have not taken into account the variation of the 3D screening parameter $q_0 a$ in function of D_e. These calculations show the competition between the effect of the position of the VHs and the value of $q_0 a$ for getting the optimum T_C, this competition depends on the compound. When the overdoping is increased, i.e. the density of free carriers increases, then $q_0 a$ increases too, and in our model this leads to a decrease in T_C. It is why for $D_e = 0$, or $p = 0.20$, we do not have the optimum T_C, and why the logarithmic law for χ_p is found in the overdoped range [27]. In the underdoped range with respect to the observed optimum T_C, (i.e. the density of free carriers decreases), $q_0 a$ decreases too, but the Fermi level goes too far away from the singularity to obtain high T_C. Our results agree completely with the experimental observations.

7 Gap Anisotropy

7.1 The Calculation

Bouvier and Bok [26] have shown that using a weakly screening electron–phonon interaction, and the band structure of the CuO_2 planes, an anisotropic superconducting gap is found.

We use the BCS equation for an anisotropic gap:

$$\Delta_{\vec{k}} = \sum_{k'} \frac{V_{kk'}\Delta_{k'}}{\sqrt{\xi_{k'}^2 + \Delta_{k'}^2}} \tag{4}$$

and instead of a constant potential as used in BCS, we choose a weakly screened attractive electron-phonon interaction potential:

$$V_{kk'} = \frac{-|g_q|^2}{q^2 + q_0^2} < 0 \tag{5}$$

where $g(q)$ is the electron–phonon interaction matrix element for $\vec{q} = \vec{k'} - \vec{k}$ and q_0 is the inverse of the screening length. We compute $\Delta_{\vec{k}}$ for two values of $\vec{k}$:

$$\Delta_A \quad \text{for } k_x a = \pi, k_y a = 0, \tag{6a}$$

$$\Delta_B \quad \text{for } k_x a = k_y a = \frac{\pi}{2}. \tag{6b}$$

We solve (4) by iteration for these two specific points of the Fermi surface, the saddle point A $(\pi, 0)$ or (1, 0) direction, and point B $(\pi/2, \pi/2)$ or (1, 1) direction. To obtain the entire dependence in the wave vector $\vec{k}$, we know from group theory considerations that $V_{kk'}$ having a four-fold symmetry, the solution Δ_k has the same symmetry, so we may use the angle Φ between the 0 axis and the $\vec{k}$ vector as a variable and expand $\Delta(\Phi)$ in Fourier series:

$$\Delta(\Phi) = \Delta_0 + \Delta_1 \cos(4\Phi + \varphi_1) + \Delta_2 \cos(8\Phi + \varphi_2) + \cdots \tag{7}$$

Further developments of the calculations and explanations about this model are presented in Ref. [26]. We obtain, for the two computed values:

$$\Delta_A = \Delta_{Max} = \Delta_0 + \Delta_1 \quad \text{and} \quad \Delta_B = \Delta_{min} = \Delta_0 - \Delta_1.$$

The gap anisotropy is important because the scattering is essentially forward, this is due to the weak screening in two dimensions. The wave vector explores a small region in k-space. The gap is important in the direction of the saddle point, due to its high density of states, and its effect is reinforced by the weak screening. But for the point B $(\pi/2, \pi/2)$ the DOS is smaller and the effect is reduced.

From our theoretical results, we find an effective coupling constant λ_{eff} in agreement with the hypothesis of the BCS weak electron-phonon coupling.

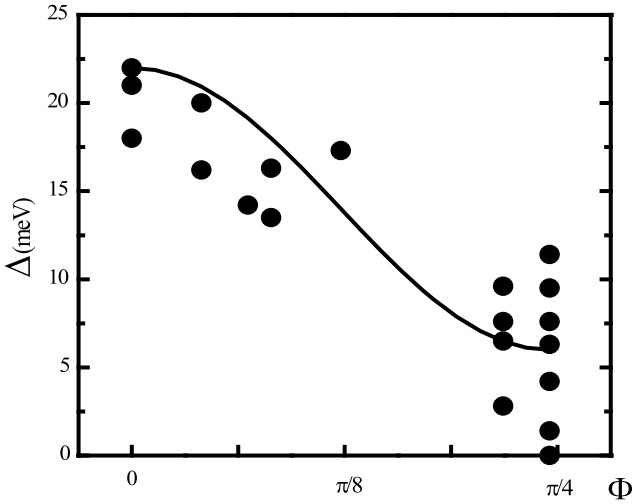

Fig. 16 Anisotropic superconducting gap. Calculation for $\Phi = 0$ and $\pi/4$. This represents a s-wave anisotropic superconducting gap with no nodes in $\Phi = \pi/4$

7.2 Results

In Fig. 16, we present the result of the iterative calculation. We thus obtain an "extended s-wave" gap and not a d-wave pair function. The order parameter is never negative in our model. Abrikosov [50] has shown, however, that if a short-range repulsive interaction (which can represent either some part of the Hubbard repulsion at the copper sites or the interaction mediated by spin fluctuations) is added, then the order parameter can vary in sign and become negative at points of the Fermi surface distant from the singularity. Such an approach may reconcile all the observations leading sometimes to s-wave and other times to d-wave symmetry of the order parameter. The fact that the order parameter is negative in certain regions of the Fermi surface explains the results of experiments showing a π phase shift of the order parameter [51].

In Fig. 17, we present the variation of the various gaps Δ_{Max}, Δ_{min} and Δ_{av} (or Δ_0) with temperature at optimum doping, i.e. for a density of holes of the order of 0.20 per CuO_2 plane. We find $T_C = 91$ K and an anisotropy ratio $\alpha = \Delta_{Max}/\Delta_{min} = 4.2$ and for the ratios of $2\Delta/k_B T_C$ the following values:

$$\frac{2\Delta_{Max}}{k_B T_C} = 6, \qquad \frac{2\Delta_{av}}{k_B T_C} = 3.7, \qquad \frac{2\Delta_{min}}{k_B T_C} = 1.4.$$

This may explain the various values of $2\Delta/k_B T_C$ observed in various experiments. The critical temperature found is $T_C = 90.75$ K as for HTSC cuprates as $Bi_2Sr_2CaCu_2O_8$ (Bi 2212), $YBa_2Cu_3O_{7-\delta}$ (Y123).

In Fig. 18, we present the same results, Δ_{Max}, Δ_{min}, Δ_{av} as a function of $E_F - E_S$ linked to the variation of doping.

We observe of course that T_C, Fig. 10, and the gaps, Fig. 18, decrease with the doping from the optimum dop-

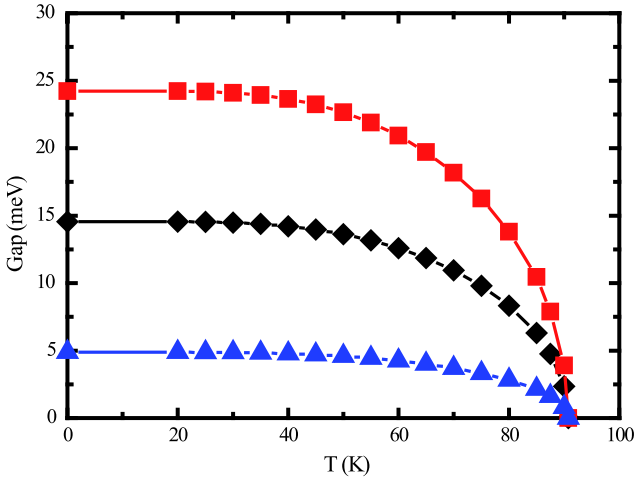

Fig. 17 Variation of the various gaps Δ_{Max}, Δ_{min} and Δ_{av} versus temperature, at the optimum doping, with the following parameters, $t = 0.2$ eV, $\hbar\omega_0 = 60$ meV, $q_0a = 0.12$, $\lambda_{eff} = 0.665$. From top to bottom: *square symbol* $= \Delta_{Max}$, *diamond symbol* $= \Delta_{av}$, *up triangle symbol* $= \Delta_{min}$

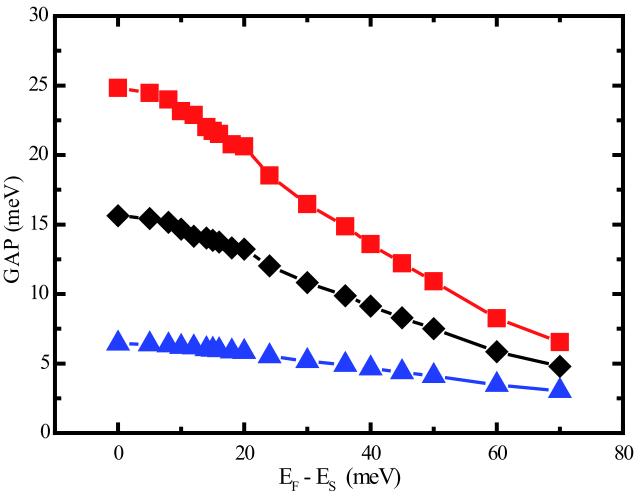

Fig. 18 Variation of the various gaps Δ_{Max}, Δ_{min}, Δ_{av} versus the doping linked to $E_F - E_S$ at $T = 0$ K. From top to bottom: *square symbol* $= \Delta_{Max}$, *diamond symbol* $= \Delta_{av}$, *up triangle symbol* $= \Delta_{min}$

ing to the overdoped region in these calculations. We obtain also an interesting result, which is the decrease of the anisotropy ratio α with doping [22, 23, 52]. This is confirmed by ARPES results.

7.3 Effect of the Screening on the Gap Anisotropy and T_C

We stress the importance of q_0a, the screening parameter, in the value of T_C and the anisotropy ratio $\alpha = \Delta_{Max}/\Delta_{min}$. We give the results of our study, in the approximation of weak screening ($q_0a < 0.2$). The results are presented in Fig. 19. We see that increasing q_0a, or, in other words, going towards a more metallic system or 3D, the anisotropy of the gap decreases. For T_C, the results are presented in Fig. 20. The

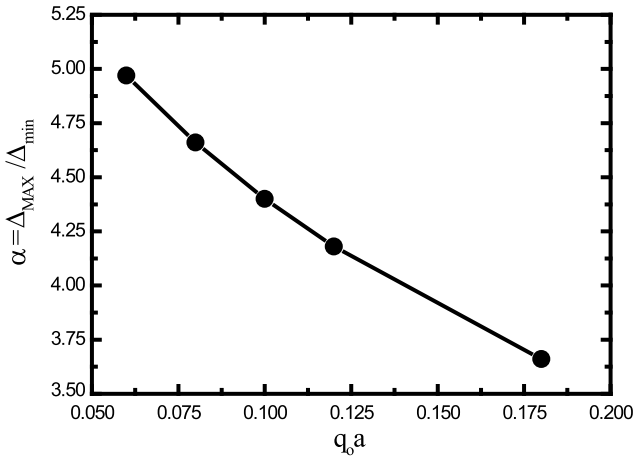

Fig. 19 The anisotropy ratio $\alpha = \Delta_{Max}/\Delta_{min}$ versus the screening parameter q_0a, detailed calculations are done in Ref. [52]

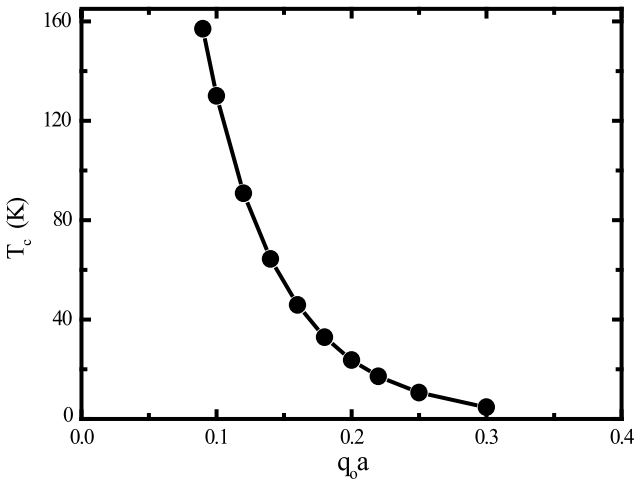

Fig. 20 T_C versus the screening parameter q_0a, detailed calculations are done in Ref. [52]

effect of increasing the screening strength is to decrease T_C. An increase of the screening can be due to the proximity of E_F to E_S where the DOS is high, and on the other side T_C is increased by the high DOS. There is a competition of the two effects to obtain the maximum T_C. It is why we have to take into account these two effects and why the experimental T_C is not maximum when $E_F = E_S$ [52].

We show that the effect of increasing q_0a is to transform the system in a metallic and more isotropic one.

8 Evidence of Lattice Involvement

Labbé and Friedel [3–5] gave an explanation for the martensitic phase transformation from the cubic to the tetragonal structure observed at low temperature in the A15 compounds of formula V_3X (X = Si, Ga, Ge, ...) or Nb_3Sn. This change of structure occurs at a temperature T_M greater

than T_C. The vanadium (V) atoms form a linear chain and an almost one dimensional approximation can be used for the d-electrons. In these conditions a VHs appears at the bottom of the band and can explain high T_C [4, 6, 7]. The electronic energy is reduced when the lattice is deformed and leads to a band type Jahn–Teller effect. This effect can explain the observed cubic to tetragonal transition at low temperature. This effect does not change T_C very much in these A15 compounds, because the role of the high DOS due to the VHs is important only for small doping (low concentration of d-electrons).

The situation is more favorable in the cuprates, which are almost bidimensional and where the VHs lies near the middle of the band. Far from or near T_C, lattice deformations, tetragonal-to-orthorhombic phase transformations, deformation of the orthorhombic phase, even martensitic phase transformations, have been observed in the cuprates in function of temperature, doping, substitution, or under strain [27, 53–57]. This leads to a competition between electronic and elastic energies. Evidence of the role of phonon in the physics of cuprates has been seen experimentally, see for example the paper of Graf et al. [58].

When the Fermi level lies close to a VHs, of energy E_S, as is the case for cuprates near optimum doping, the situation could be unstable and a small distortion increases the distance $E_F - E_S$ and decreases strongly the electronic energy.

We propose a different scenario in most of these 2D compounds. When the lattice in the CuO_2 plane is quadratic, the four saddle points correspond to the same electronic energy E_S and the VHs is fourfold degenerate. Due to the doping, and then to the effect of decreasing the temperature, the lattice becomes orthorhombic (rectangular unit cell). The degeneracy is lifted and we hope to obtain two VHs at different energy E_{S1} and E_{S2} corresponding to the saddle points along k_x and k_y in reciprocal space.

$$E_k = -2t(1+\beta)\cos X - 2t\cos Y + 4t'\cos X\cos Y + D_e \tag{8}$$

Using the twofold degenerate electronic dispersion, (8), where βt represents the difference in the interaction with the first neighbors in the x and y direction, we calculate the DOS versus energy, represented on Fig. 21. In optimal conditions the Fermi level could lie between E_{S1} and E_{S2}. E_F is then between these energy levels of high DOS in a dip, itself of a smaller but sufficiently high DOS, the lattice is stabilized. No more phase transformation could be possible, at lower temperature this situation favors the BCS condensation into a superconducting phase instead of a lattice transformation, leading to high T_C due to the high DOS.

The goal for experimentalists will be to find the optimal parameters (doping, strain, temperature, ...) to lead the sample to such situation that it condensates when E_F is pinned in its dip in order to obtain a very high T_C.

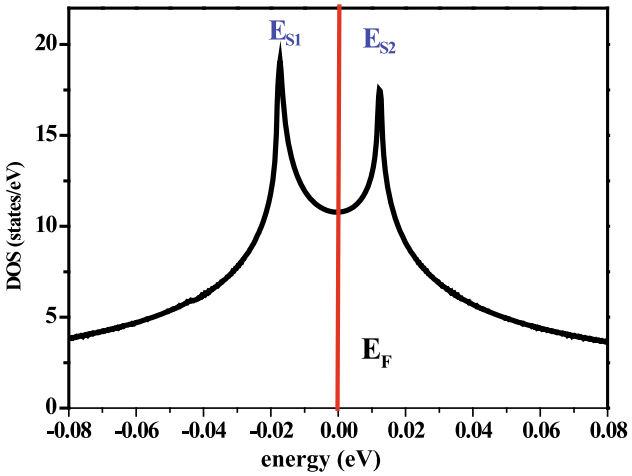

Fig. 21 Density of states in the orthorhombic phase

We want to indicate in favor of the electron-lattice interaction that de Gennes and Deutscher [59] proposed a model valid in the underdoped regime based on the idea that if two holes occupy two adjacent copper sites, a contraction of the Cu–O–Cu band occurs. This increases significantly the transfer integral between the Cu and this can lead to the formation of bound hole pairs.

9 Conclusion

Strong correlations are probably the dominant factor in the underdoped region. But in the optimum and overdoped regions, we have shown that the experimental observations may be explained by electron–phonon or electron–lattice interaction coupled with the Van Hove scenario, both in the normal and superconducting states. The existence of VHs close to the Fermi level is now well established experimentally and this fact must be taken into account in any physical description of the properties of high T_C superconducting cuprates.

Acknowledgements Jacqueline Bouvier personally met Professor Friedel for the first time the day of her thesis defense. He came, invited by one of my researcher friends, and he stayed during the cocktail. She adds: I was very impressed by his long and slim figure and his glittering eyes with strength emerging from him. After this first meeting, we met sometimes in his home to discuss our respective work. He was always very interested and always took into account my own words and capacities. I was very touched by his gentleman behavior regarding me. Until now, we are corresponding to exchange the ideas submitted in our papers. I want to deeply thank him for his intellectual interest in our work and express how I am admiring his lifelong work.

References

1. Labbé, J., Barišić, S., Friedel, J.: Phys. Rev. Lett. **19**, 233 (1962)
2. Labbé, J., Friedel, J.: J. Phys. Radium **27**, 153 (1966)

3. Labbé, J., Friedel, J.: J. Phys. (Paris) **27**, 153 (1966)
4. Labbé, J., Friedel, J.: J. Phys. (Paris) **27**, 303 (1966)
5. Labbé, J., Friedel, J.: J. Phys. (Paris) **27**, 708 (1966)
6. Labbé, J., Barišić, S., Friedel, J.: Phys. Rev. Lett. **19**, 1039 (1967)
7. Barišić, S., Labbé, J.: J. Phys. Chem. Solids **28**, 2477 (1967)
8. Labbé, J.: Phys. Rev. Lett. **158**, 647 (1967)
9. Labbé, J.: Phys. Rev. **158**, 655 (1967)
10. Labbé, J.: Phys. Rev. Lett. **172**, 451 (1968)
11. Friedel, J.: Transition metals. In: Ziman, J.M. (ed.) Physics of Metals I. Electrons. Cambridge University Press, Cambridge (1969)
12. Barišić, S., Labbé, J., Cyrot-Lackmann, F.: J. Phys. (Paris) **30**, 955 (1969)
13. Labbé, J., van Reuth, E.C.: Phys. Rev. Lett. **24**, 1232 (1970)
14. Barišić, S., Labbé, J., Friedel, J.: Phys. Rev. Lett. **25**, 919 (1970)
15. Barišić, S.: Phys. Rev. B **5**, 932 (1972)
16. Testardi, L.R., Bateman, T.B., Reed, W.A., Chirba, V.G.: Phys. Rev. Lett. **15**, 250 (1965)
17. Testardi, L.R., Bateman, T.B.: Phys. Rev. **154**, 402 (1967)
18. Bednorz, J.G., Müller, K.A.: Z. Angew. Phys. B **64**, 189 (1986)
19. Barišić, S., Batistic, I., Friedel, J.: Europhys. Lett. **3**, 1231 (1987)
20. Van Hove, L.: Phys. Rev. **89**, 1189 (1953)
21. Labbé, J., Bok, J.: Europhys. Lett. **3**, 1225 (1987)
22. Bok, J., Bouvier, J.: Van Hove scenario for high T_C superconductors. In: Bussmann-Holder, A., Keller, H. (eds.) High T_C Superconductors and Related Transition Metal Oxides, pp. 35–41. Springer, Berlin (2007)
23. Bouvier, J., Bok, J.: Electron–phonon Interaction in the high-T_C cuprates in the framework of the Van Hove scenario. Adv. Condens. Matter Phys. **2010**, 472636 (2010). doi:10.1155/2010/472636
24. Ino, A., Kim, C., Nakamura, M., Yoshida, Y., Mizokawa, T., Fujimori, A., Shen, Z.X., Takeshita, T., Eisaki, H., Uchida, S.: Phys. Rev. B **65**, 094504 (2002)
25. Lee, P.A., Nagaosa, N., Wen, X.-G.: Rev. Mod. Phys. **78**, 17 (2006)
26. Bouvier, J., Bok, J.: Physica C **249**, 117 (1995)
27. Bouvier, J., Bok, J.: Physica C **288**, 217 (1997)
28. Koike, Y., Iwabuchi, Y., Hosoya, S., Kobayashi, N., Fukase, T.: Physica C **159**, 105 (1989)
29. Bardeen, J., Cooper, L.N., Schrieffer, J.R.: Phys. Rev. **108**, 1175 (1957)
30. Morel, P., Anderson, P.W.: Phys. Rev. **125**, 1263 (1962)
31. Cohen, M.L., Anderson, P.W.: In: Douglass, D.H. (ed.) Superconductivity in d and f Band Metals. AIP, New York (1972)
32. Ginzburg, V.: Contemp. Phys. **33**, 15 (1992)
33. Force, L., Bok, J.: Solid State Commun. **85**, 975 (1993)
34. Batlogg, B., Kourouklis, G., Weber, W., Cava, R.J., Jayaraman, A., White, A.E., Short, K.T., Rupp, L.W., Rietman, E.A.: Phys. Rev. Lett. **59**, 912 (1987)
35. Crawford, M.K., Kunchur, M.N., Farneth, W.E., McCarron, E.M. III, Poon, S.J.: Phys. Rev. B **41**, 282 (1990)
36. Keller, H.: In: Müller, K., Bussmann-Holder, A. (eds.) Structure and Bonding, vol. 114, p. 143. Springer, Heidelberg (2005)
37. Tsuei, C.C., Newns, D.M., Chi, C.C., Pattnaik, P.C.: Phys. Rev. Lett. **65**, 2724 (1990)
38. Pattnaik, P.C., Kane, C.L., Newns, D.M., Tsuei, C.C.: Phys. Rev. B **45**, 5714 (1992)
39. Newns, D.M., Tsuei, C.C., Pattnaik, P.C., Lane, C.L.: Comments Condens. Matter Phys. **15**, 273 (1992)
40. Hlubina, R., Rice, T.M.: Phys. Rev. B **51**, 9253 (1995)
41. Olson, C.G., Liu, R., Lynch, D.W., List, R.S., Arko, A.J., Veal, B.W., Chang, Y.C., Jiang, P.Z., Paulikas, A.P.: Phys. Rev. B **42**, 381 (1990)
42. Schlesinger, Z., et al.: Phys. Rev. Lett. **67**, 2741 (1991)
43. Kubo, Y., Shimakawa, Y., Manako, T., Igarashi, H.: Phys. Rev. B **43**, 7875 (1991)
44. Matthey, D., Gariglio, S., Giovannini, B., Triscone, J.-M.: Phys. Rev. B **64**, 024513 (2001)
45. Balakirev, F.F., Betts, J.B., Migliori, A., Ono, S., Ando, Y., Boebinger, G.S.: Nature **424**, 912 (2003)
46. Bok, J., Bouvier, J.: Physica C, Supercond. **403**, 263 (2004)
47. Ong, N.P.: Phys. Rev. B **43**, 193 (1991)
48. Williams, G.V.M., Tallon, J.L., Haines, E.M., Michalak, R., Dupree, R.: Phys. Rev. Lett. **78**, 721 (1997)
49. Cooper, J.R., Loram, J.W.: J. Phys. I Fr. **6**, 2237 (1996)
50. Abrikosov, A.A.: Physica C **244**, 243 (1995)
51. Tsuei, C.C., Kirtley, J.R., Hammerl, G., Mannhart, J., Raffy, H., Li, Z.Z.: Phys. Rev. Lett. **93**, 187004 (2004)
52. Bouvier, J., Bok, J.: J. Supercond. **10**, 673 (1997)
53. Kyomen, T., Oguni, M., Itoh, M., Yu, J.D.: Phys. Rev. B **60**, 6821 (1999)
54. Egami, T.: Essential role of the lattice in the mechanism of high temperature superconductivity. In: Bussmann-Holder, A., Keller, H. (eds.) High T_C Superconductors and Related Transition Metal Oxides, pp. 103–129. Springer, Berlin (2007)
55. Toby, B.H., Egami, T., Jorgensen, J.D., Subrmanian, M.A.: Phys. Rev. Lett. **64**, 2414 (1990)
56. Oyanagi, H.: Lattice effects in high temperature superconducting cuprates revealed by X-ray absorption spectroscopy. In: Bussmann-Holder, A., Keller, H. (eds.) High T_C Superconductors and Related Transition Metal Oxides, pp. 253–258. Springer, Berlin (2007)
57. Lee, J., Fujita, K., McElroy, K., Slezak, J.A., Wang, M., Aiura, Y., Bando, H., Ishikado, M., Masui, T., Zhu, J.-X., Balatsky, A.V., Eisaki, H., Uchida, S., Davis, J.C.: Nature **442**, 546 (2006)
58. Graf, J., d'Astuto, M., Jozwiak, C., Garcia, D.R., Saini, N.L., Krisch, M., Ikeuchi, K., Baron, A.Q.R., Eisaki, H., Lanzaral, A.: Phys. Rev. Lett. **100**, 227002 (2008)
59. Deutscher, G., de Gennes, P.G.: C. R. Phys. **8**, 937 (2007)